A NEW MODULATION SCHEME FOR RAPID BLIND TIMING ACQUISITION USING DIRTY TEMPLATE APPROACH FOR UWB SYSTEMS

Mourad Ouertani[1,4], Huilin Xu[2], Liuqing Yang[2], Hichem Besbes[3] and Ammar Bouallègue[4]

[1] Institut Supérieur d'Informatique, ISI, Tunisia, ouertani.mourad@gmail.com

[2] Dept. of Electrical & Computer Engr., University of Florida, Gainesville, FL 32601, USA, xuhl@ufl.edu, lqyang@ece.ufl.edu

[3] Research Unit TECHTRA, Ecole Supérieure des Communications de Tunis, Sup'Com, Tunisia, hichem.besbes@supcom.rnu.tn

[4] Laboratoire SysCom, Ecole Nationale d'Ingénieurs de Tunis, ENIT, Tunisia, ammar.bouallegue@enit.rnu.tn

ABSTRACT

Timing acquisition is one of the major challenges in ultra-wideband (UWB) communications. The timing with dirty template (TDT) approach is an attractive technique for UWB systems, which is characterized by its low complexity and fast acquisition in the data-aided (DA) mode. However, in the non-data-aided (NDA) mode, the performance of this approach degrades due to the random symbol effect. In this paper, we propose to overcome this issue by adopting orthogonal pulse-shape modulation (PSM) proposed in [1], [2]. Our algorithm uses a train of alternating orthogonal Hermite pulses to modulate the transmitted symbols. The application of the TDT approach to the proposed scheme shows an enhancement of synchronization speed in the NDA mode. Simulations confirm performance improvement of TDT with the proposed modulation relative to the original TDT in terms of the mean square error (MSE) and the acquisition probability.

Index Terms— Synchronization, timing

1. INTRODUCTION

Ultra-wideband (UWB) is a promising technology for short-range indoor wireless communications with low complexity transceivers. Timing synchronization is a major challenge in UWB systems (see e.g., [3]). Timing with dirty template (TDT) was developed for rapid synchronization of UWB signals [3]. This technique relies on correlating adjacent symbol-long segments of the received waveform. TDT is operational with arbitrarily transmitted symbol sequence. When training symbols (pilots) are affordable, the performance of the TDT synchronizer can be improved by adopting a data-aided mode [3]. However, the training sequence results in an overhead which reduces the bandwidth and energy efficiencies.

To improve the energy efficiency and the synchronization performance of the original TDT, we propose a novel modulation scheme which employs alternating orthogonal UWB pulses. During each symbol duration, one of the two orthogonal waveforms $p_1(t)$ and $p_2(t)$ is used as the pulse shaper. When $p_1(t)$ and $p_2(t)$ are two Hermite pulses with consecutive orders, the pulse shapers at the receiver, which are the second-order derivatives of $p_1(t)$ and $p_2(t)$ are still orthogonal [1]. With this modulation scheme, we develop a new TDT synchronizer structure. Compared with the original TDT synchronizers, this new structure improves the system energy efficiency by only slightly increasing the transceiver complexity. Simulation results show that this new TDT synchronizer can achieve a lower mean square error (MSE) and a higher acquisition probability than the original TDT in both nondata-aided (NDA) and data-aided (DA) modes.

2. SYSTEM MODEL

Consider an impulse radio UWB system, where every information symbol is transmitted over a T_s period that consists of N_f frames. During each frame of duration T_f, a data-modulated pulse $p(t)$ of duration $T_p \ll T_f$ is generated to excite the transmit antenna. The transmitted signal is

$$v(t) = \sqrt{\mathcal{E}} \sum_{k=0}^{\infty} s_k \cdot p_T(t - kT_s) \;, \tag{1}$$

where $\mathcal{E}$ is the energy per pulse, s_k is the kth information symbol taking values $\{\pm 1\}$ and $p_T(t)$ denotes the transmitted symbol-level waveform:

$$p_T(t) = \sum_{n=0}^{N_f-1} c_{ds}(n) \cdot p'(t - nT_f - c_{th}(n)T_c), \tag{2}$$

where T_c is the chip duration and the transmit waveform $p(t)$ becomes its first-order derivative $p'(t)$ due to the differentiation effect of the transmit antenna [4].

Notice that $p_T(t)$ can be regarded as the symbol-level pulse shaper which accounts for the time-hopping (TH) and/or direct-sequence (DS) spreading via $c_{th}(n)$ and $c_{ds}(n)$, respectively. Without loss of generality, we assume that the symbol duration T_s is an integer multiple of T_p.

Let $g(t - \tau_0)$ denote the equivalent multipath channel with propagation delay τ_0. Then, the received waveform can be

1-4244-0728-1/07/$20.00 ©2007 IEEE

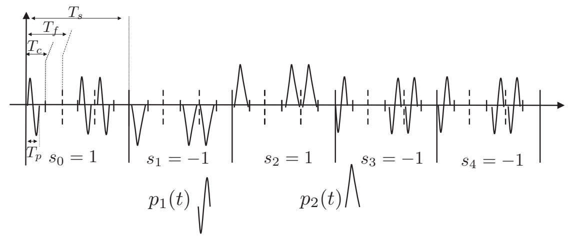

Fig. 1. The new modulation scheme and the TH code $[0, 1, 0]$.

expressed as:

$$r(t) = \sqrt{\mathcal{E}} \sum_{k=0}^{\infty} s_k \cdot p_R(t - kT_s - \tau_0) + \eta(t) \;, \qquad (3)$$

where $\eta(t)$ represents the bandpass-filtered zero-mean additive white Gaussian noise (AWGN) with power spectral density (PSD) $\mathcal{N}_0/2$, and $p_R(t)$ denotes the aggregate symbol-level received waveform:

$$p_R(t) = \sum_{n=0}^{N_f-1} c_{ds}(n) \cdot p''(t - nT_f - c_{th}(n)T_c) \star g(t), \quad (4)$$

where $\star$ denotes convolution and the second-order derivative of $p(t)$ is due to the differentiation effect of the receive antenna [4].

3. TDT WITH ORTHOGONAL PULSES

Our novel timing scheme employs two orthogonal Hermite pulses $p_1(t) = h_n(t)$ and $p_2(t) = h_{n+1}(t)$ with the same pulse duration T_p, where $h_n(t)$ is the nth-order Hermite pulse proposed in [4]. Therefore, not only $p_1(t)$ and $p_2(t)$ but also their first or second-order derivatives form an orthogonal pulse pair.

Unlike the original DA-TDT where the polarity of the symbols is alternated, in our scheme, the UWB pulse shaper is alternately chosen from $p_1(t)$ and $p_2(t)$, each conveying one information symbol. The pulse shaper is changed according to the following pattern $[p_1(t), p_2(t), p_2(t), p_1(t)]$ or its circulation (see Fig. 1). The symbol-level transmitted and received waveforms are denoted by $p_{T1}(t)$ and $p_{R1}(t)$ when the pulse $p_1(t)$ is employed, and by $p_{T2}(t)$ and $p_{R2}(t)$ otherwise.

At the receiver, the TDT algorithms are employed to estimate the channel delay τ_0. Following the idea of dirty templates [3], these algorithms rely on pairs of successive groups each of duration T_s. The groups in each pair then serve as templates for each other to generate the symbol-rate samples as follows:

$$x(k;\tau) = \int_0^{T_s} r(t + 2kT_s + \tau) r(t + (2k-1)T_s + \tau) dt$$
$$\forall k \in [1, +\infty),$$

where τ is the candidate time shift.

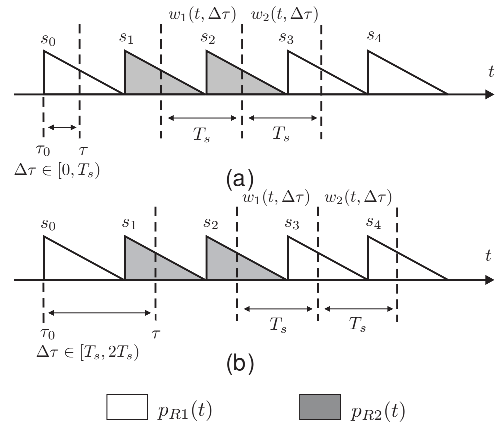

Fig. 2. The received waveform.

Let $\chi(k;\Delta\tau)$ denote the noise-free part of $x(k;\Delta\tau)$, $\Delta\tau := \tau - \tau_0$. Without loss of generality, we set $k = 1$ for notational simplicity. The noise-free part of the correlation of the two T_s-long segments $w_1(t;\Delta\tau)$ and $w_2(t;\Delta\tau)$ taken from the received waveform at the starting time $(T_s + \tau_0 + \Delta\tau)$ is given by (see Fig. 2)

$$\chi(1;\Delta\tau) = \int_0^{T_s} w_1(t;\Delta\tau) w_{\,2}(t;\Delta\tau) dt. \qquad (5)$$

Fig. 2 repents the noise-free parts of the received waveforms of the first five symbols. For illustrative purpose, $p_R(t)$ is plotted as a triangle with the maximum non-zero support of T_s and the frame-level repetition is ignored. Notice that every $p_{Ri}(t)$, $i \in \{1, 2\}$, can be partitioned into two segments $v_i^a(t;\Delta\tau)$ and $v_i^b(t;\Delta\tau)$ (see Fig. 3):

$$v_i^a(t;\Delta\tau) = \begin{cases} 0, & t \in [0, T_s - [\Delta\tau]_{T_s}) \\ p_{Ri}(t - T_s + [\Delta\tau]_{T_s}), & t \in [T_s - [\Delta\tau]_{T_s}, T_s) \end{cases},$$

and

$$v_i^b(t;\Delta\tau) = \begin{cases} p_{Ri}(t + [\Delta\tau]_{T_s}), & t \in [0, T_s - [\Delta\tau]_{T_s}) \\ 0, & t \in [T_s - [\Delta\tau]_{T_s}, T_s) \end{cases},$$

where $[x]_y$ is the modulo operation of x with basis y.

The waveforms $v_i^a(t;\Delta\tau)$ and $v_i^b(t;\Delta\tau)$ constitute a whole symbol-level received waveform $p_{Ri}(t)$ as:

$$p_{Ri}(t) = v_i^a(t + T_s - [\Delta\tau]_{T_s};\Delta\tau) + v_i^b(t - [\Delta\tau]_{T_s};\Delta\tau). \qquad (6)$$

Since the non-zero supports of $v_i^a(t;\Delta\tau)$ and $v_i^b(t;\Delta\tau)$ do not overlap, the following always holds true:

Lemma 1 *When the non-zero support of $p_R(t)$ is upper bounded by T_s, we have*

$$\int_0^{T_s} v_n^a(t;\Delta\tau) v_m^b(t;\Delta\tau) dt = 0, \; n, m \in \{1, 2\}.$$

In addition, we invoke the following assumption on the propagation channel (see e.g., [5]):

(as) The channel arrivals are equally spaced with spacing T_p.

With this assumption and the fact that the received pulses $p_1''(t)$ and $p_2''(t)$ are orthogonal, it readily follows that

Lemma 2 *The correlation between any symbol-long segment conveying pulse* $p_1''(t)$ *and any symbol-long segment conveying pulse* $p_2''(t)$ *is zero; that is*

$$\int_0^{T_s} v_1^{\alpha}(t;\tau)v_2^{\beta}(t;\tau)dt = 0,\ \alpha,\beta \in \{a,b\}.$$

Though **Lemma 1** and **2** can be employed to simplify (5), the simplification also relies on the transmitted pulse pattern; i.e., what sequence of pulses $p_1''(t)$ and $p_2''(t)$ are involved in $\chi(1;\Delta\tau)$. Next, we will consider different patterns separately.

3.1. First case: $\Delta\tau \in [0, T_s)$

In this case, $w_1(t;\Delta\tau)$ and $w_2(t;\Delta\tau)$ involve symbols s_1, s_2 and s_3 (see Fig. 2(a)). Correspondingly, the received pulse pattern is $[p_2''(t), p_2''(t), p_1''(t)]$. As a result, equation (5) becomes:

$$\begin{aligned}\chi(1;\Delta\tau) = &\int_0^{T_s} \left(s_1 v_2^b(t;\Delta\tau) + s_2 v_2^a(t;\Delta\tau)\right) \\ &\times \left(s_2 v_2^b(t;\Delta\tau) + s_3 v_1^a(t;\Delta\tau)\right) dt,\ \Delta\tau \in [0, T_s).\end{aligned} \tag{7}$$

Using **Lemma 1** and **Lemma 2**, $\chi(1;\Delta\tau)$ becomes:

$$\chi(1;\Delta\tau) = \int_0^{T_s} s_1 s_2 (v_2^b(t;\Delta\tau))^2 dt. \tag{8}$$

Accordingly, the absolute value of $\chi(1;\Delta\tau)$ can be equivalently expressed as:

$$|\chi(1;\tau)| = \int_0^{T_s} \left(v_2^b(t;\Delta\tau)\right)^2 dt \triangleq \mathcal{E}_b(\Delta\tau). \tag{9}$$

It is worthy to note that $\mathcal{E}_b(\Delta\tau)$ decreases as $[\Delta\tau]_{T_s}$ increases. Therefore, for $\Delta\tau \in [0, T_s)$, $|\chi(1;\Delta\tau)|$ is a decreasing function.

3.2. Second case: $\Delta\tau \in [T_s, 2T_s)$

In this case, the received pulse sequence is $[p_2''(t), p_1''(t), p_1''(t)]$, since $w_1(t;\Delta\tau)$ and $w_2(t;\Delta\tau)$ now involve symbols s_2, s_3 and s_4 as shown in Fig. 2(b). Equation (5) can be expressed as follows:

$$\begin{aligned}\chi(1;\Delta\tau) = &\int_0^{T_s} \left(s_2 v_2^b(t;\Delta\tau) + s_3 v_1^a(t;\Delta\tau)\right) \\ &\times \left(s_3 v_1^b(t;\Delta\tau) + s_4 v_1^a(t;\Delta\tau)\right) dt,\ \Delta\tau \in [T_s, 2T_s).\end{aligned} \tag{10}$$

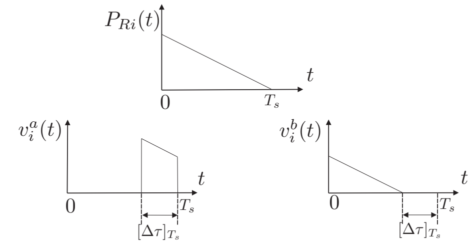

Fig. 3. The T_s-long signal segments.

Using **Lemma 1** and **Lemma 2**, $\chi(1;\Delta\tau)$ becomes:

$$\chi(1;\Delta\tau) = \int_0^{T_s} s_3 s_4 (v_1^a(t;\Delta\tau))^2 dt. \tag{11}$$

Accordingly, the absolute value of $\chi(1;\Delta\tau)$ can be equivalently expressed as:

$$|\chi(1;\Delta\tau)| = \int_0^{T_s} \left(v_1^a(t;\Delta\tau)\right)^2 dt := \mathcal{E}_a(\Delta\tau). \tag{12}$$

Since $\mathcal{E}_a(\Delta\tau)$ increases as $[\Delta\tau]_{T_s}$ increases, $|\chi(1;\Delta\tau)|$ is an increasing function for $\Delta\tau \in [T_s, 2T_s)$.

We notice that $|\chi(1,\Delta\tau)|$ approaches $\mathcal{E}_a(T_s) = \mathcal{E}_b(0)$, when $\Delta\tau$ approaches $2T_s$. Also, $|\chi(1;\Delta\tau)|$ is continuous at $\Delta\tau = T_s$, because we have $|\chi(1,\Delta\tau)| = 0$ when $\Delta\tau = T_s$ and $|\chi(1,\Delta\tau)|$ approaches 0, when $\Delta\tau$ approaches T_s. In addition, $|\chi(1,\Delta\tau)|$ is a periodic function of $\Delta\tau$ with a period of $2T_s$. That means $|\chi(1,\Delta\tau)| = |\chi(1, 2T_s + \Delta\tau)|$, $\forall\Delta\tau$. Therefore, $|\chi(1,\Delta\tau)|$ reaches its minimum when $[\Delta\tau]_{2T_s} = T_s$, and reaches its maximum when $[\Delta\tau]_{2T_s} = 0$. This result leads to a timing synchronizer based on the sample mean of the symbol-rate sample $|x(k;\Delta\tau)|$.

3.3. TDT Synchronizer

It is interesting to note that with the proposed orthogonal pulse modulation, the TDT algorithm does not depend on the transmitted symbols. Therefore, a blind acquisition can be built which relies on that the sample mean of $|x(k;\Delta\tau)|$ reaches its maximum when $[\Delta\tau]_{2T_s} = 0$. The proposed modulation associated with the TDT synchronization approach is expected to achieve a better acquisition performance than that of the original TDT in the NDA mode.

Next, let us build the realistic TDT synchronizer with the proposed orthogonal pulses.

Proposition 1: Blind TDT can be accomplished even when TH codes are present and the UWB multipath channel is unknown, using "dirty" T_s-long segments of the received waveform as follows:

$$\hat{\tau}_0 = \arg \max_{\tau\in[0,\ 2T_s)} y(M;\tau) \tag{13}$$

$$y(M;\tau) = \frac{1}{M}\sum_{k=1}^{M} \left| \int_0^{T_s} r(t + 2kT_s + \tau) r(t + (2k-1)T_s + \tau) dt \right|.$$

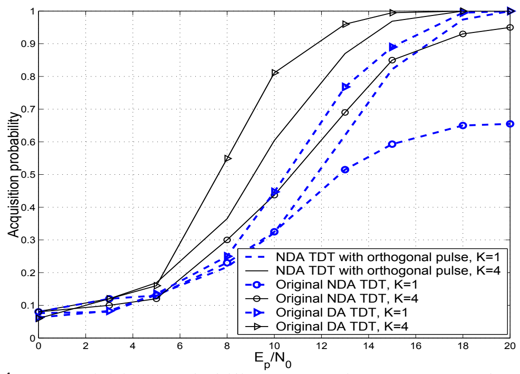

Fig. 4. Acquisition probability comparison: proposed TDT vs. original DA and NDA TDT.

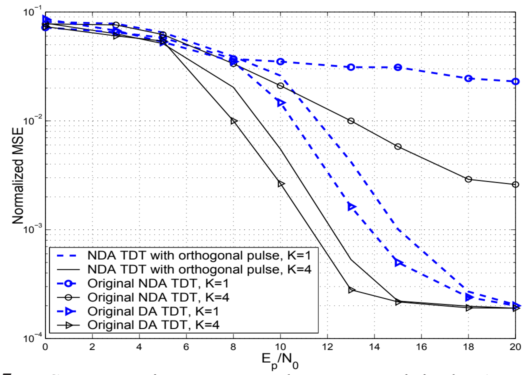

Fig. 5. MSE comparison: proposed TDT vs. original DA and NDA TDT.

As with the original TDT, the new TDT synchronizer requires only symbol-rate samples. Additionally, with the orthogonal Hermite pulses, this synchronizer enjoys rapid acquisition relying on a minimum of four symbols using a pulse sequence of $[p_1(t), p_2(t), p_2(t), p_1(t)]$.

4. SIMULATIONS

In this section, we will evaluate the performance of the proposed TDT synchronizer with simulations. We select the orthogonal pulses $p_1(t)$ and $p_2(t)$ as two consecutive Hermite pulses with duration $T_p \approx 0.8ns$. The simulations are performed in a modified Saleh-Valenzuela channel [6, 7] with parameters $\Lambda = 0.0233$ (1/ns), $\lambda = 2.5(1/\text{ns})$, $\Gamma = 7.1$ns and $\gamma = 4.3$ns. The maximum channel delay spread of the channel is about 31ns. Each symbol duration contains $N_f = 32$ frames with $T_f = 32$ns. We compare the performance of the new TDT synchronizer with that of the original TDT in both NDA and DA modes. In all simulations, only frame-level coarse timing is performed.

First, let us compare the acquisition probability of the proposed TDT synchronizer with the original NDA and DA TDT algorithms. With the orthogonal pulse modulation, our new synchronizer can remarkably outperform the original NDA TDT algorithm and achieve a comparable performance to the DA TDT algorithm. In Fig. 5, we compare the mean square error (MSE) for all three TDT synchronizers. The MSE is normalized by the square of the symbol duration T_s. The performance of our modulation in NDA mode is comparable to that of the original DA TDT synchronization algorithm. Even without training symbol sequence, our new TDT synchronizer can greatly outperform the original NDA TDT especially when K is small. Obviously, this performance improvement is enabled at the price of higher complexity by alternating the pulse shaper.

5. CONCLUSION

In this paper, we establish a new timing scheme based on the dirty template synchronization algorithm for UWB radio system. With the pulse-shape modulation, the transmitter alternately chooses the pulse shaper from two consecutive order Hermite pulses in a predefined order. Both the theoretical analysis and simulation results show that even without training symbols, our new TDT synchronizer can enable a performance better than the original TDT in NDA mode and comparable to the original TDT in DA mode.

6. REFERENCES

[1] L. B. Michael, M. Ghavami and R. Kohno, "Multiple pulse generator for ultra-wideband communications using Hermite polynomial based orthogonal pulses," in *Proc. 2002 IEEE Conf. on Ultra Wideband Systems and Tech.*, Baltimore, MD, May 21–23, 2002, pp. 47–51.

[2] M. Pinchas and B. Z. Bobrovsky, "Orthogonal Laguerre polynomial pulses for ultra-wideband communications," in *Proc. IEEE International Workshop on Ultra-Wideband Systems*, Oulu, Finland, June 2003.

[3] L. Yang and G. B. Giannakis, "Timing Ultra-Wideband signals with dirty templates," *IEEE Trans. on Communications*, vol. 53, no. 11, pp. 1952–1963, November 2005.

[4] T. P. Montoya and G. S. Smith, "A study of pulse radiation from several broad-band loaded monopoles," *IEEE Trans. Antennas Propagat.*, vol. 44, no. 8, pp. 1172–1182, August 1996.

[5] S. Aedudodla, S. Vijayakumaran, and T. F. Wong, "Acquisition of direct-sequence transmitted reference ultra-wideband signals," *IEEE Journal on Selected Areas in Communications*, vol. 24, no. 4, pp. 759–765, April 2006.

[6] R. J.-M. Cramer, R. A. Scholtz, and M. Z. Win, "Evaluation of an ultra-wide-band propagation channel," *IEEE Trans. on Antennas and Propagation*, vol. 50, no. 5, pp. 561–570, May 2002.

[7] A. A. M. Saleh and R. A. Valenzuela, "A statistical model for indoor multipath propagation," *IEEE Journal on Selected Areas in Communications*, vol. 5, no. 2, pp. 128–137, February 1987.